electronics

Article

Method for Fault Diagnosis of Track Circuits Based on a Time–Frequency Intelligent Network

Feitong Peng [1,*] and Tangzhi Liu [2]

[1] School of Information Science and Engineering, Chongqing Jiaotong University, Chongqing 400074, China
[2] College of Traffic & Transportation, Chongqing Jiaotong University, Chongqing 400074, China; liutangzhi@cqjtu.edu.cn
* Correspondence: pengfeitong@mails.cqjtu.edu.cn

Abstract: In response to the limitations posed by noise interference in complex environments and the narrow focus of existing diagnosis methods for jointless track circuit faults, an innovative approach is put forward in this study. It involves the application of the continuous wavelet transform (CWT) for signal preprocessing, along with the integration of a deep belief network (DBN) and a genetic algorithm (GA) to improve the least-squares support vector machine (LSSVM) model for intelligent time–frequency fault diagnosis. Initially, the raw induced voltage signals are transformed using continuous wavelet transformation resulting in wavelet time–frequency representations that combine temporal and spectral information. Subsequently, these time–frequency representations are fed into the deep belief networks, which perform semi-supervised dimensionality reduction and feature extraction, thereby uncovering distinct fault characteristics in the track circuit. Finally, the genetic algorithms are employed to improve the kernel function and penalty factor parameters of the least-squares support vector machine, thus establishing an optimal DBN-GA-LSSVM diagnostic model. Experimental validation demonstrates the effectiveness of the proposed time–frequency intelligent network model by leveraging the advantages of deep belief networks in hierarchical feature extraction and the superior performance of the least-squares support vector machine in addressing high-dimensional pattern recognition problems with limited samples. The achieved accuracy rate on the testing dataset reaches an impressive 99.6%. Consequently, this comprehensive approach provides a viable solution for data-driven track circuit fault diagnosis.

Keywords: fault diagnosis; jointless track circuit; continuous wavelet transform; least-squares support vector machine; genetic algorithm

Citation: Peng, F.; Liu, T. Method for Fault Diagnosis of Track Circuits Based on a Time–Frequency Intelligent Network. *Electronics* **2024**, *13*, 859. https://doi.org/10.3390/electronics13050859

Academic Editors: Ahmed Abu-Siada, Shuiqing Xu, Darong Huang, Ke Zhang and Zheren Zhu

Received: 5 January 2024
Revised: 18 February 2024
Accepted: 21 February 2024
Published: 23 February 2024

1. Introduction

In recent times, high-speed railways have swiftly emerged as the favored mode of transportation due to their wide distribution and convenient travel. To guarantee the secure functioning of railway networks, the real-time, accurate, and efficient diagnosis and timely detection of high-speed railway system faults has emerged as an imminent issue in need of resolution. As the fundamental element of a railway signal system, the track circuit can accurately represent the real-time running state of the railway in a lightweight way. Within this framework, it is of great strategic significance to realize the real-time and accurate detection and preemptive identification of track circuit faults for reducing maintenance costs, improving operation efficiency, and ensuring the driving safety of high-speed railway networks.

ZPW-2000A is a widely used jointless frequency-shift track circuit technology. Through a variety of sensors connected to the track, such as transformers, receivers, and attenuators, ZPW-2000A can transmit multi-dimensional signals from the track in real time to achieve the functions of occupancy inspection, broken rail inspection, and ground vehicle communication. However, once the track circuit fails, the field technicians usually need to rely on a frequency-shift test table to test the data from the attenuator, the cable simulation network disk, and the cable, or use a microcomputer monitoring system to test the data from each part.

Advancements in deep learning have led to the effective integration of artificial intelligence algorithms in system health diagnosis and prognosis [1]. When applied to track circuits, these algorithms contribute to the development of intelligent and lightweight diagnostic technology. Within the realm of track circuit fault diagnosis, scholars from both national and international backgrounds have put forth numerous novel approaches based on neural networks, data mining, and algorithm optimization. They are dedicated to integrating artificial intelligence with fault diagnosis technology, aiming to enhance the precision and promptness of fault diagnosis. Bruin T D et al. [2] proposed a recurrent neural network with long-term and short-term memory, and realized fault diagnosis after training the network with real track data. Zhao et al. [3] analyzed the dynamic response of a seamless track circuit within a complex electromagnetic environment, and proposed a method rooted in the finite-difference time domain to effectively handle the transmission line component. To address the nonlinear equation in the track circuit, the Thevenin theorem and the state variable method were employed, thereby offering a theoretical foundation for analyzing the interference in track circuits. Recognizing the impact of various stochastic and uncertain factors, such as adverse operating conditions, intricate equipment configurations, and the diverse causes of faults in track circuitry, Zang et al. [4] introduced the set pair analysis theory. Drawing upon the methodology of set pair analysis, the uncertainty degree was expressed through mathematical framework, and the connection number expression between the indices and the running state was systematically described. Through this systematic approach, a comprehensive and precise evaluation of the state of the track circuit was successfully achieved. The efficiency of this diagnostic method is limited by expert technology and space–time constraints, which leads to difficulty in obtaining real-time early warnings of railway operation faults, and thus it is challenging to fulfill the requirements needed for accurately repairing fault states. Lu et al. [5] proposed an intelligent diagnostic model grounded in convolutional neural networks to swiftly anticipate fault data. Gou et al. [6] employed the continuous wavelet transform for preprocessing fault signals, reducing the training difficulty of neural networks. Cao et al. [7] devised a fault diagnosis technique for track circuits, employing least-squares support vector machines. In comparison to backpropagation neural networks, this classifier, grounded in least-squares support vector machines, demonstrates superior diagnostic accuracy while requiring less training time. Additionally, a portion of researchers are devoted to enhancing the accuracy and interpretability of deep learning models. Zheng et al. [8] improved the predictive accuracy and robustness of deep belief networks through a genetic algorithm-optimized particle swarm optimization algorithm (GAPSO). Chen et al. [9] devised a hybrid approach that integrates quantitative and qualitative methodologies, harnessing the synergistic advantages of a neural fuzzy system. By harmoniously merging the intrinsic strengths of fuzzy logic and neural networks, this approach significantly amplifies the accuracy and precision of track circuit fault diagnosis. Li et al. [10] suggested a fault diagnosis methodology that integrates a rough set theory reduction model with Bayesian network structure learning. Through the dual driving forces of data and knowledge, the accuracy of neural networks is substantially enhanced. Gao et al. [11] combined least-squares support vector machines with particle swarm optimization, further improving the accuracy of fault diagnosis through the optimization of kernel function parameters. With the continuous emergence of these new approaches, real-time, thorough, and precise diagnosis of track circuit faults is gradually being realized. Meanwhile, fault diagnosis in other fields also has referential significance, such as high-speed trains [12–15] and centrifugal pumps. Ahmad S et al. [16] extracted fault-related discriminant features from kurtogram images. Ullah N et al. [17] proposed a fault diagnosis framework based on wavelet coherence analysis and deep learning.

Track circuit fault diagnosis steps are generally divided into signal processing, feature extraction, and fault classification. Signal processing refers to the use of various signal analysis methods to analyze and process the state signals collected during circuit operation. The CWT can obtain the characteristic signals of fault information [18]. For feature extraction and pattern classification, the deep learning algorithm uses the super feature extraction ability of the deep neural network model, and then uses the classification model to classify the sample data, which is the frontier processing method of fault diagnosis. However, the existing deep learning methods also have defects. For example, Zhang K et al. [19] used one-dimensional convolution for fault feature extraction. These methods directly process one-dimensional vibration time-series signals without considering the frequency-domain information in the signals. Therefore, this paper uses the CWT to perform time–frequency domain processing on track circuit signals and convert one-dimensional signals into two-dimensional time–frequency images. In order to promote the development of track circuit diagnostic technology and achieve more efficient and accurate fault diagnosis, an integrated fault diagnosis framework, named DBN-GA-LSSVM, is designed in this study. This framework employs a DBN for hierarchical feature learning to extract features from fault signals preprocessed by the wavelet transform. An LSSVM is utilized as the classification layer for fault classification to further enhance the performance of the LSSVM, which employs a genetic algorithm to improve the penalty factor and kernel function. The CWT captures instantaneous features of signals through time–frequency domain analysis, the DBN extracts advanced feature representations through deep learning, the GA optimizes parameters through global searches, and the LSSVM deals with nonlinear relationships. This fusion method overcomes the limitation of traditional methods in complex circuit fault diagnosis, and improves the modeling and optimization performance of the time-varying and nonlinear characteristics of the system. Overall, this method brings a new perspective and efficient solution to the field of uninsulated track circuit fault diagnosis.

2. Track Circuit Fault Diagnosis Network Design

2.1. Overview of the DBN-GA-LSSVM Diagnosis Framework

The proposed framework for the fault diagnosis of the time–frequency intelligent track circuit is depicted in Figure 1 of this paper. The framework is segmented into four components and is executed in accordance with the subsequent steps.

1. The creation of a ZPW-2000A track circuit voltage simulation model, implemented in the Simulink software MATLAB R2022a, is initiated. This model is utilized to reflect the fault modes of the track circuit, and a corresponding voltage fault dataset is generated.
2. The initial dataset undergoes continuous wavelet transformation to unveil the time–frequency characteristics inherent in the voltage signals.
3. The DBN model is utilized to extract distinctive features from the wavelet spectrograms, while the LSSVM is employed as a classifier for fault diagnosis.
4. Optimization of the LSSVM parameters is achieved through the application of a genetic algorithm (GA), and the refined model's effectiveness is assessed using an independent test set.

2.2. Generation of the Dataset

2.2.1. Modeling of the ZPW-2000A

The ZPW-2000A track circuit is composed of two integral segments: the primary track and the secondary track. Spanning from the transmission point to the reception point, this track circuit configuration encompasses essential components, including a transmitter, transmission cables, matching transformers, rails, tuning units, hollow coils, compensating capacitors, and receivers, as illustrated in Figure 2. The electrical insulation section consists of two types of tuning units, TU1 and TU2, a hollow coil SVA, and a segment of rail. The compensating capacitance on the main track is the capacitance of the main track. The impedance Z_{TU1}, Z_{TU2}, and Z_{SVA} correspond to the equivalent impedances of tuning units TU1, TU2, and the hollow coil SVA, respectively.

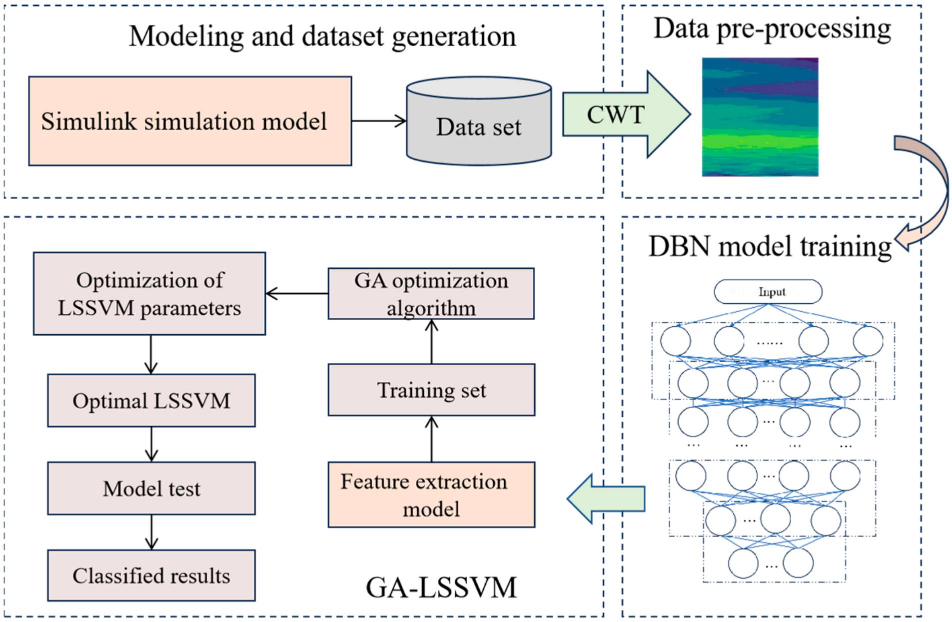

Figure 1. Time–frequency intelligent network flow chart.

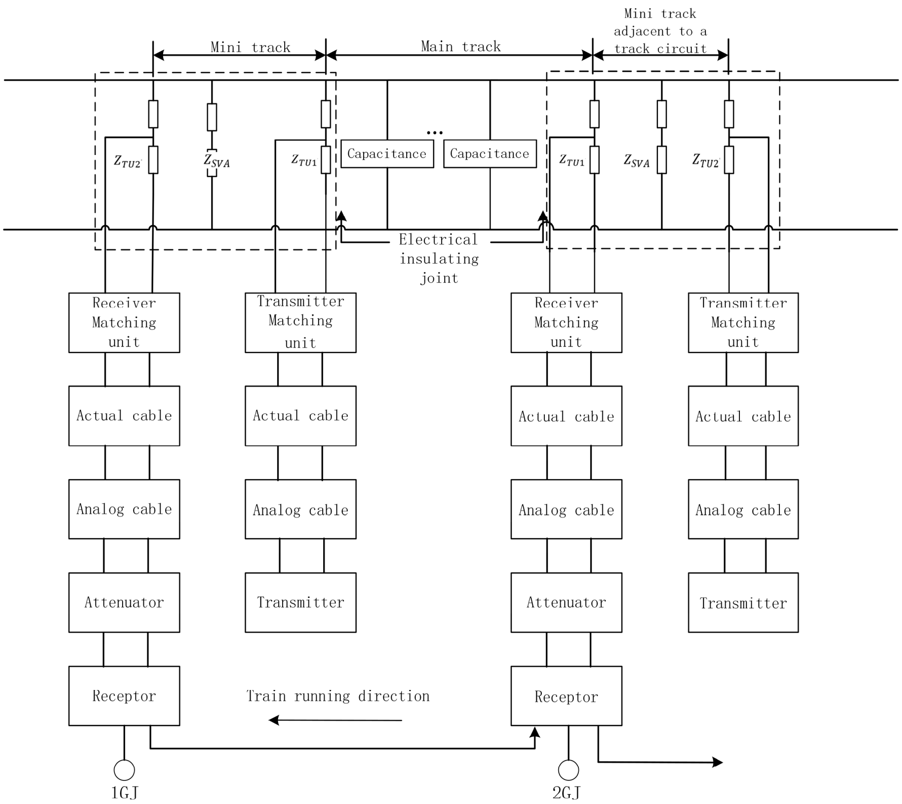

Figure 2. Configuration of ZPW-2000A.

The occurrence of failure in track circuits can be inferred by the variations in voltage levels within the circuit. However, some faults may require on-site judgment from maintenance personnel based on their own experience. In this study, a comprehensive analysis of the causes and consequences of faults in various track circuit equipment is conducted, resulting in the identification of 20 typical track circuit faults; the patterns of these faults and their respective impacts are presented in Table 1.

Table 1. Typical fault classification table of a track circuit.

Fault Number	Failure Mode	Failed Part
F1	normal	-
F2 F3	the sending voltage is large the sending voltage is small	transmitter
F4 F5 F6	the analog network capacitance is small the analog network inductance is small SPT cable fault	transmitting cable
F7	matching transformer fault	transmitter matching transformer
F8 F9 F10	TU1 failure SVA failure TU2 failure	transmitter tuning area
F11 F12 F13	the ballast resistance is large the ballast resistance is small compensation capacitor fault	rail line
F14 F15 F16	TU1 failure SVA failure TU2 failure	receiver tuning area
F17	matching transformer fault	receiving-end matching transformer
F18 F19 F20	SPT cable fault the analog network capacitance is small the inductance of the analog network is small	seismic cable

2.2.2. Time–Frequency Visualization of the CWT

The continuous wavelet transform (CWT) is a mighty time–frequency analysis method that provides a comprehensive analysis of signals at different scales [20]. The voltage signals in railway circuits can be regarded as one-dimensional time series, with the amplitude corresponding to each sampling point represented on the y-axis, and the time or sampling points represented on the x-axis [21]. Different sections of the railway circuit employ carrier signals of varying frequencies. Railway circuits are typically subjected to complex operating environments, affected by factors such as temperature variations, humidity, and electromagnetic interference. These factors give rise to complex nonlinear, non-stationary, and stochastic characteristics in the signals, thereby increasing the difficulty of fault diagnosis. Traditional approaches that directly feed voltage signals into neural networks encounter challenges in capturing inherent features, leading to constraints on the precision and adaptability of fault diagnosis. To overcome this limitation, the present study adopts the continuous wavelet transform (CWT) to preprocess the raw voltage signals. This application aims to unveil the time–frequency characteristics embedded within the signals while mitigating the impact of noise signals. Consequently, this methodology enhances the efficacy of fault diagnosis in railway circuits.

By utilizing variable windows to transform the signals, the CWT offers different resolutions at different time periods and frequencies, enabling better capture of local time–frequency characteristics in the signals [22]. This makes the CWT suitable for capturing induced voltage non-stationary signals in railway circuits, where time and frequency variations are present.

The CWT dissects the original signal into a sequence of wavelet series, denoted as $\varphi_{a,b}(t)$. This dissection is achieved by manipulating the wavelet basis function, $\varphi(t)$, through translations and scalings. In this context, a defines the scale parameter, determining the localization of the wavelet time–frequency window within the frequency domain. On the other hand, b governs the transformation, determining the placement of the time-domain wavelet time–frequency window. The expression of continuous wavelet transformation is as follows:

$$\varphi_{a,b}(t) = \frac{1}{\sqrt{|a|}}\varphi\left(\frac{t-b}{a}\right) \tag{1}$$

For the induced voltage signal $u(t)$, the CWT expression is as follows:

$$W_u(a,b) = \frac{1}{\sqrt{|a|}}\int_{-\infty}^{\infty} u(t)\varphi^*\left(\frac{t-b}{a}\right)dt \tag{2}$$

In this context, $W_u(a,b)$ represents the wavelet coefficient; φ^* represents the conjugate of the wavelet basis function.

Through the application of the CWT, the original time-domain signal undergoes a transformation into the scale-domain representation. Equation (3) gives the conversion relationship between scale and frequency:

$$f_u = \frac{f_c \times f_s}{a}, \tag{3}$$

within this equation, f_u denotes the signal frequency, f_s represents its sampling rate, and f_c signifies the central frequency of the wavelet.

Based on Formula (3), the frequency distribution corresponding to the signal's scale can be determined, culminating in the acquisition of the wavelet time–frequency graph for the signal. This diagram vividly portrays the temporal and spectral characteristics of the signal, effectively illustrating its frequency–time–amplitude relationship. In this study, feature extraction hinges on the wavelet time–frequency representation of the signal, facilitating the exploration of anomaly detection in track circuit voltage.

Taking the rail-in voltage as an example, the time-domain signal diagram of the rail voltage can be obtained through Formulas (1)–(3), as shown in Figure 3. The sampling rate is 2500 Hz, and the sampling time is 10 ms.

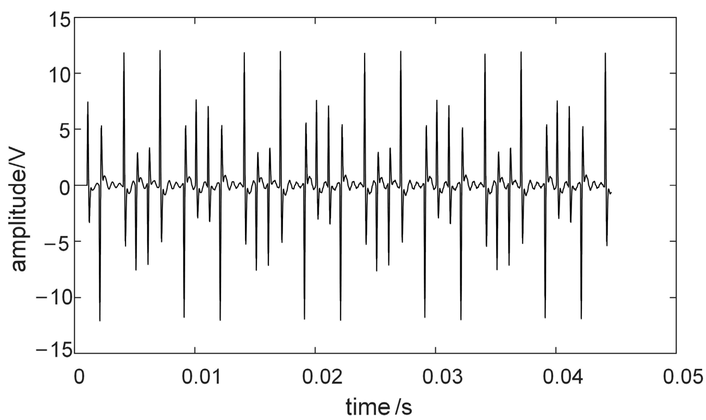

Figure 3. Track voltage time-domain signal diagram.

2.3. Deep Belief Network

Due to the lack of actual fault data in the field of track circuitry, the diagnosis model must be able to effectively extract the data feature changes involved in the problem under certain data conditions. A DBN well solves the problem of feature extraction pre-learning and deep network training being prone to falling into local optimal solutions. A DBN effectively overcomes problems such as the slow training speed of top-level classifiers, the insufficient feature extraction of neural network data, and the forward pre-training and supervised reverse tuning methods' tendencies to fall into local extremum.

A deep belief network (DBN) is a probabilistic generative model composed of layered hidden units, including restricted Boltzmann machines (RBMs) [23]. Figure 4 depicts the typical configuration of a DBN. The RBM comprises a visible layer (v) and a hidden layer (h), with bidirectional connections between the units of each layer. The neurons within each layer operate independently, where the visible layer neuron can be expressed as $v = \{v_1, v_2, \cdots, v_n\}$, and the hidden layer neuron as $h = \{h_1, h_2, \cdots, h_m\}$. The joint probability density function between the input layer neuron v and the hidden layer neuron h is expressed as follows:

$$E(v,h) = -\sum_{i=1}^{n} v_i a_i - \sum_{j=1}^{m} h_j b_j - \sum_{i=1}^{n} \sum_{j=1}^{m} h_i v_i w_{ij} j, \tag{4}$$

among which w_{ij} represents the connection weight between the visible layer unit i and the hidden layer unit j, while a_i and b_j denote the offsets of the visible and hidden layer units, respectively.

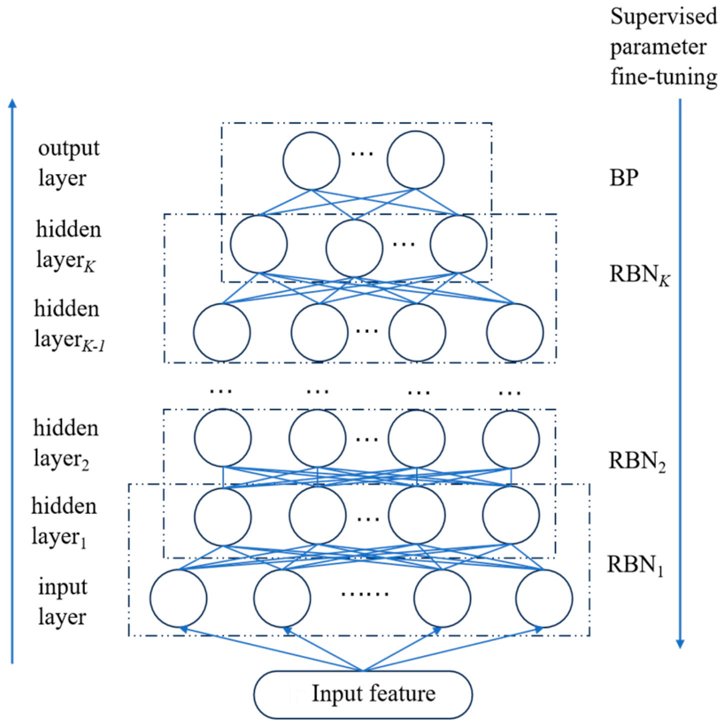

Figure 4. DBN structure and training process.

The DBN method is employed for fault feature extraction in the track circuit, involving two main stages: pre-training and fine-tuning. During pre-training, various types of track circuit fault data undergo unsupervised training in layer one of the RBM of the deep confidence network. The trained model's output serves as the input to subsequent layers, and layer by layer, greedy learning continues until the output layer yields track circuit fault characteristics.

The fine-tuning phase incorporates supervised learning, where the output results are compared with label data. The error backpropagation algorithm is utilized to reverse-train the DBN, optimizing its parameters. The DBN's advantage lies in its ability to extract advanced features through layer-by-layer training, further enhancing model parameters in the fine-tuning stage with supervised learning. This approach effectively extracts valuable feature information from track circuit fault data, providing crucial support for fault diagnosis and prediction.

2.4. Least-Squares Support Vector Machine

To address the classification conundrum of high-dimensional data with limited samples, this paper uses the LSSVM [24] as the DBN top-level classifier model. The LSSVM technique utilizes the least-squares method to convert the inequality constraints of support vector machines (SVMs) into equality constraints. This transformation results in the training process being streamlined into solving linear equations, effectively simplifying the algorithm's complexity. Firstly, the following classification problem-solving equation is established:

$$\min_{\boldsymbol{\omega},b,\mathbf{e}} F(\boldsymbol{\omega}, b, \mathbf{e}) = \frac{1}{2}\boldsymbol{\omega}^{\mathrm{T}}\boldsymbol{\omega} + \frac{1}{2}\gamma\sum_{i=1}^{m} \mathbf{e}_i^2, \tag{5a}$$

$$\text{s.t. } y_i\left[\boldsymbol{\omega}^T\varphi(\boldsymbol{x}_i) + b\right] = 1 - \mathbf{e}_i, \tag{5b}$$

$$\gamma > 0, i = 1, 2, \cdots, m, \tag{5c}$$

where $\mathbf{e}$ is the deviation vector; γ represents the weight, also known as the penalty factor; $\boldsymbol{\omega}$ is the weight coefficient vector of the LSSVM; y_i is the category label; b is the threshold; φ is a kernel function, which makes the samples linearly separable in higher-dimensional space. The Lagrange function is introduced to solve the maximum condition of this function, and the classification formulation of the LSSVM is as follows:

$$y(\boldsymbol{x}) = \operatorname{sign}\left[\sum_{i=1}^{m} \alpha_i y_i K(\boldsymbol{x}, \boldsymbol{x}_i) + \mathrm{b}\right], \tag{6}$$

where $\boldsymbol{x}$ is the track circuit fault feature vector extracted using the DBN; $K(\boldsymbol{x}, \boldsymbol{x}_i)$ represents the kernel function, and specifically, the radial basis kernel function is selected in this paper, and its definition is given in Formula (7), where σ^2 is the kernel function parameter.

$$K(\boldsymbol{x}_i, \boldsymbol{x}_j) = \exp\left(-||\boldsymbol{x}_i - \boldsymbol{x}_j||2\sigma^2\right), \tag{7}$$

Because the classification accuracy of an LSSVM model is greatly affected by penalty factor γ and kernel function parameter value σ^2, the penalty factor γ controls the penalty error beyond the error sample; the larger the penalty factor γ is, the stronger the adaptability is, and the more over-fitting is prone to occur. The smaller the γ is, the lower the complexity of the model is, and the more prone it is to under-fitting. The kernel function parameter σ^2 affects the dimension of the output space. The traditional LSSVM method usually uses a fixed γ, while a GA can optimize the selection of the most suitable kernel function to adapt to different data patterns and problems. The genetic algorithm can find the optimal solution in the parameter combination through global search and optimization in the parameter space to improve the performance and effect of the LSSVM model.

2.5. Genetic Algorithm

The genetic algorithm (GA) is based on the principle of "survival of the fittest", akin to the fundamental concept elucidated in Darwin's theory of evolution. As with other evolutionary algorithms, a GA employs fundamental operators such as selection, crossover, and mutation [25], known for their global optimization performance and robustness. In this paper, a GA is employed to acquire the improved kernel function and penalty factor parameters of the LSSVM. The accuracy of classification in the test set serves as the metric for fitness evaluation in acquiring the optimal parameters of the LSSVM. Figure 5 shows the algorithm optimization flow chart.

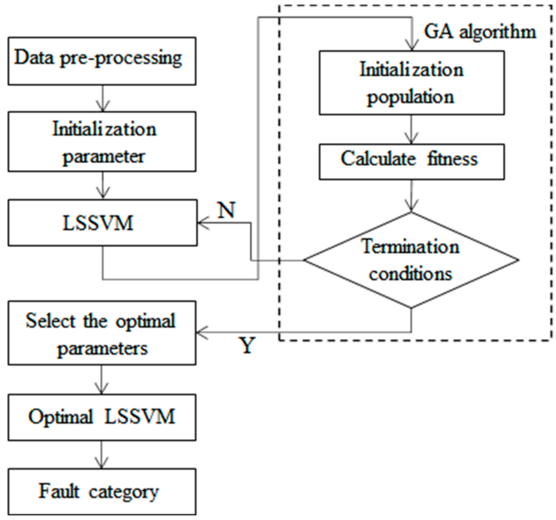

Figure 5. GA-LSSVM diagnosis flow chart.

3. Experiment

3.1. Experimental Setup and Evaluation Index

In this experiment, a Simulink model is employed to simulate the track circuit, utilizing six selected monitoring variables as the original feature set: M1 (transmitted voltage), M2 (cable output voltage at the transmitter), M3 (rail surface voltage at the transmitter end), M4 (rail surface voltage at the receiver end), M5 (cable input voltage at the receiver), and M6 (rail input voltage). Table 2 presents the field-test data in comparison to the calculated results, where E1 represents the absolute error, and E2 denotes the relative error. The track circuit simulation model developed in this study exhibits high accuracy, with a maximum relative error of 4.80% observed at the rail surface voltage of the sending end when comparing the simulation results to field-test data.

Table 2. Comparison of field-test data and simulation results.

Feature	Simulative Value/V	Measured Value/V	E1/%	E2/%
M1	104	104	0	0
M2	34.28	34.65	0.37	1.07
M3	2.97	3.12	0.15	4.80
M4	2.61	2.61	0	0
M5	20.19	20.51	0.32	1.58
M6	2.3	2.24	0.06	2.60

Aiming at the fault mode summarized in Table 1, after analyzing the monitoring parameters of the signal centralized monitoring system, this paper takes six voltage monitoring quantities as the feature set of the track circuit fault data, which are sending/receiving voltage, sending/receiving matching voltage, and sending/receiving track surface voltage. Among these, the data sample under normal operating conditions of the track circuit can be obtained through routine operation of the track circuit, and other fault samples need to establish a simulation model for the track circuit to acquire the corresponding fault sample data by changing the impedance value of the fault area. Since the track circuit fault dataset has a range of different sizes, to further enhance the network's data processing and accelerate convergence, the dataset is uniformly normalized and preprocessed to make the data distributed in the [0, 1] interval. The post-normalized track circuit data samples undergo a partitioning process into distinct sets for comprehensive analysis and evaluation. Specifically, the datasets are categorized into a training set, a validation set, and a testing set. Dataset quality is critical to deep learning. For 20 types of faults, 50 sets of training data are selected to ensure that the model has enough training samples for different types of faults and improve the model's adaptability to various fault situations. A total of 1000 sets of fault data further increase the diversity and coverage of the data. It is helpful for the model to train various fault conditions, thus improving the robustness andaccuracy of the model. Furthermore, 5 sets of validation data are chosen for each fault type, culminating in a combined total of 100 sets. Lastly, for the testing phase, 10 sets of data are procured for each type of fault, yielding a comprehensive total of 200 sets of fault data.

3.2. Time–Frequency Visualization of Continuous Wavelet Transformation

The CWT is used to extract time–frequency features from the original signal. Taking the rail-in voltage as an example, the scale range of the CWT is set to 1~6, and the Morlet wavelet function is selected as the basis function. The results of the transformation are shown in Figure 6; the abscissa is time, and the ordinate is frequency. The time–frequency features of 7800 original signals are extracted, respectively, and the time series is uniformly converted into a time–frequency image with a size of 28×28 pixels, which can fully describe the changes in signals in the time domain and frequency domain. Such representation is conducive to the training of neural network models, which ultimately leads to the improvement of convergence performance. Part of the feature extraction results are shown in Figure 7.

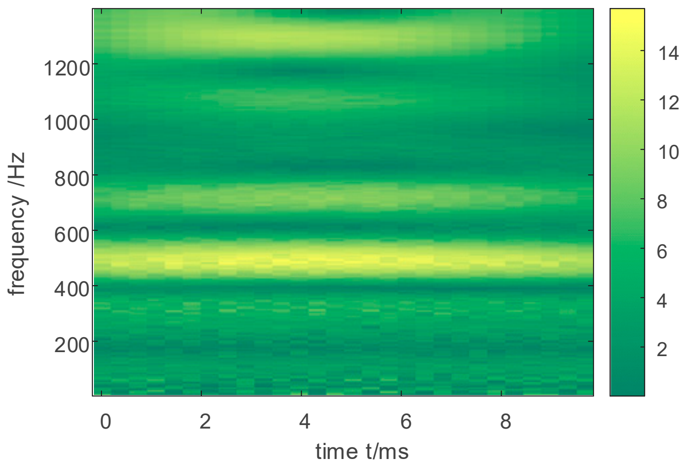

Figure 6. Wavelet time–frequency diagram of voltage signals.

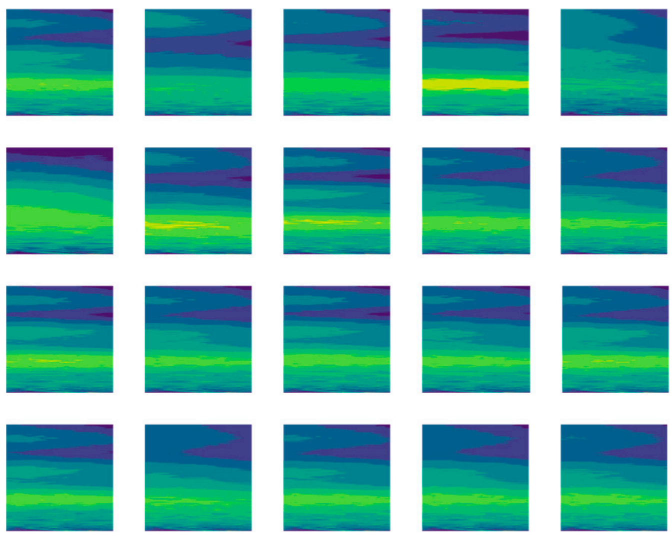

Figure 7. Time–frequency diagram feature set.

3.3. DBN-Based Fault Diagnosis Results

In this experiment, the deep belief network (DBN) serves as the feature extractor for fault signals. The input signals are the voltage time–frequency images obtained through continuous wavelet transformation, as discussed in the preceding section. The output of the DBN is a set of characteristic samples representing faults. The structure of the DBN employed in this study consists of four layers: 784-128-64-20. Each layer is responsible for learning features at different levels of abstraction. In order to optimize the weights of the DBN, it utilizes a gradient descent optimizer known as Stochastic Gradient Descent (SGD), in which the initial learning rate is specified as 0.01; during the training process, 1000 iterations are performed, with each iteration utilizing a batch size of 10 training samples. The original dataset comprises 1000 sample sets, which are randomly shuffled prior to training. In addition, 100 sample sets are reserved for validation, and another 200 sample sets are reserved for testing, ensuring a comprehensive evaluation of the model's performance.

In the presentation of the training results, it is evident that the DBN model trained without wavelet transformation (as shown in Figure 8a) exhibits a relatively fast convergence of training accuracy. However, it may suffer from unstable training accuracy. On the other hand, the DBN model trained with wavelet-transformed time–frequency images as inputs (as shown in Figure 8b) achieves a training accuracy of 93.96% after 1000 iterations. The validation accuracy is 93.50%, and the testing accuracy is 92.00%, highlighting the excellent performance of this model on both the training and validation sets. Further examination of the confusion matrices (as shown in Figure 9a,b) allows us to compare the classification performance of the DBN model with and without wavelet processing. The findings evince that the DBN model trained with wavelet transformation exhibits clearer classification results in the confusion matrix, indicating the positive role of wavelet transformation in improving the model's classification accuracy. This further confirms the effectiveness of wavelet transformation in time–frequency image processing, enabling the DBN to capture fault signal features more effectively and enhance its performance in fault-type classification tasks. Therefore, this experiment not only emphasizes the DBN's ability to extract features in a layered manner but also underscores the crucial role of wavelet transformation in fault signal processing. These findings provide strong support for the utilization of deep learning in fault diagnosis, highlighting the significance of wavelet transformation.

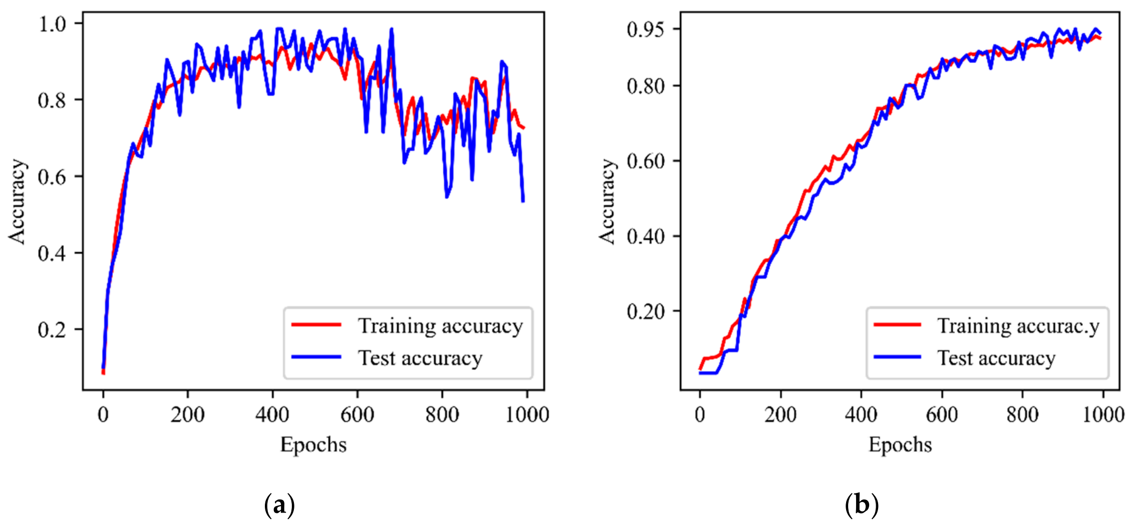

Figure 8. DBN training accuracy: (**a**) without wavelet transformation; (**b**) with wavelet transformation.

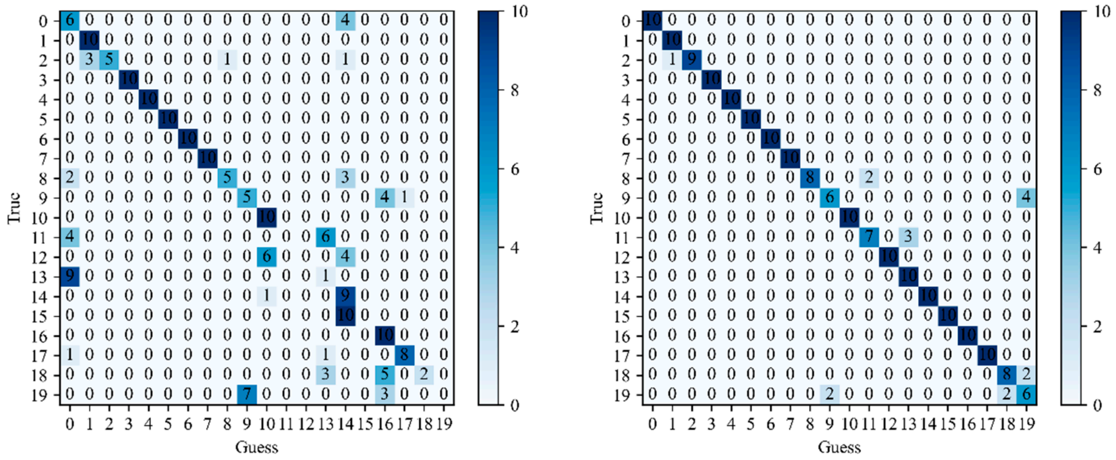

(**a**) (**b**)

Figure 9. Confusion matrix of the DBN training results: (**a**) without wavelet transformation; (**b**) with wavelet transformation.

The high-level features extracted with the DBN serve as the input for establishing a fault classification model using the LSSVM. The LSSVM uses the least-squares method to transform the training process of an SVM into solving linear equations, which simplifies the intricacy of the algorithm and performs well in dealing with small sample problems. In Figure 10a,b, the output of the feature extraction layer of the DBN model obtained by using the wavelet transform and not using the wavelet transform is shown, respectively, and the t-SNE clustering algorithm is used for visualization. Obviously, before using wavelet transformation, the feature extraction layer of the DBN fails to capture the abstract features of data well. However, by introducing wavelet transformation, the model can more effectively learn the spatio-temporal features in the data, thereby enhancing the performance of the DBN-LSSVM classification model. In the visualization results in Figure 10, the outputs of different DBN layers are displayed and t-SNE is applied to reduce the dimension and visualization. With the superposition of the number of network layers, the visualization results show a clearer and more compact classification effect.

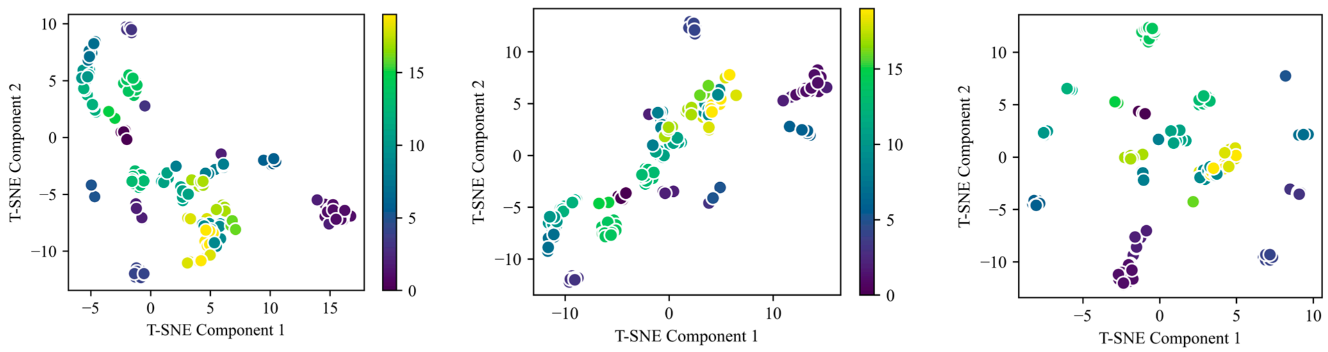

(**a**) (**b**) (**c**)

Figure 10. DBN feature extraction visualization: (**a**) first layer; (**b**) second layer; (**c**) third layer.

3.4. Genetic Algorithm Optimization for the LSSVM

In this section, a well-trained DBN with the third layer exhibiting superior feature extraction capabilities has been obtained. In this study, the DBN is utilized as a feature extractor, with its high-level features serving as inputs to the LSSVM model, aiming to enhance its performance. Furthermore, the efficacy of the LSSVM model is intricately tied to the judicious selection of its parameters. A genetic algorithm, a powerful optimization method, is employed to explore the parameter space and identify optimal solutions. The genetic algorithm's parameters include an initial population size of 50, 100 iterations, a mutation rate of 0.1, and a crossover rate of 0.4. The upper and lower boundaries for the kernel function parameters are set at 0 and 0.6, respectively, while the regularization parameters are bound between 0 and 10. Figure 11 illustrates the optimization process curve of the genetic algorithm for the LSSVM. The classification accuracy after genetic algorithm optimization reaches 99.6%. The optimized LSSVM parameters for the kernel function and regularization are found to be 0.0258 and 8.817, respectively. Figure 12 illustrates the confusion matrix of the fault diagnosis classification layer utilizing the optimized LSSVM model on the testing dataset. Compared to the singular DBN model prior to optimization, the optimized model exhibits improved recognition of fault characteristics and fault classification. Moreover, the classification accuracy on the testing dataset achieves a perfect score.

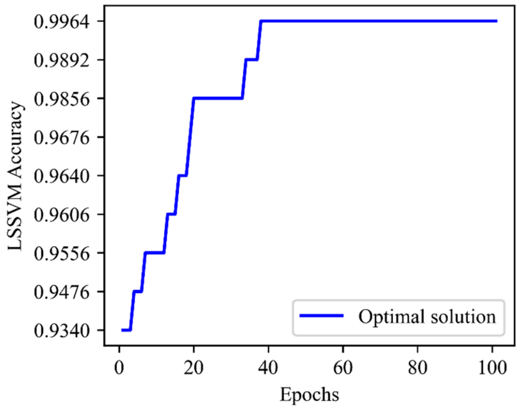

Figure 11. Fitness curve of GA optimization.

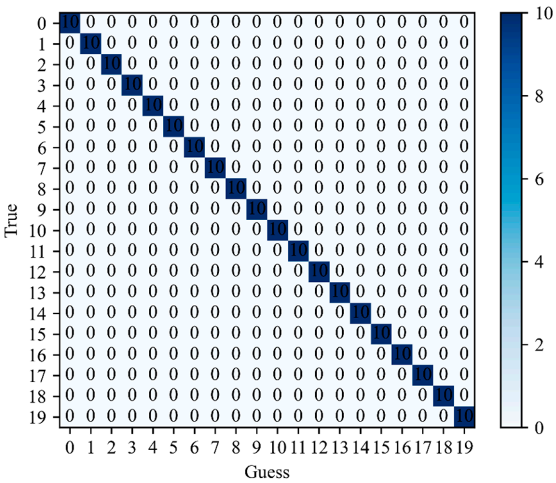

Figure 12. Confusion matrix of track circuit fault diagnosis.

3.5. Results of Fault Diagnosis Using DBN-GA-LSSVM

To conduct a thorough evaluation of the DBN-GA-LSSVM model's overall performance, a comparative analysis was undertaken against various fault diagnosis models on a dedicated test set. The suite of diagnostic models we considered encompasses diverse approaches, including deep belief networks, multi-layer perceptrons, convolutional neural networks, and backpropagation neural networks. Essential performance metrics, such as accuracy on the test set and associated training times, were scrutinized.

Table 3 vividly illustrates that the proposed DBN-GA-LSSVM model outshines its counterparts in terms of classification accuracy. Capitalizing on the robust feature extraction capabilities of the DBN and the parameter optimization prowess facilitated by the GA for the LSSVM, the model not only surpasses the accuracy of MLP and BP neural networks but also exhibits a 1.8% accuracy improvement over the CNN model. Moreover, it achieves these performance gains while significantly reducing the training time by a noteworthy 75%.

Table 3. Results of fault diagnosis from five models.

Model	Accuracy/%	Time/s
DBN	92.00	50.65
MLP	91.21	30.13
CNN	97.80	283.5
BP	91.31	28.33
DBN-GA-LSSVM	99.60	70.18

In this study, the accuracy and time required under the same training conditions are used to evaluate the performance of the model. The training process of traditional methods such as MLP mainly depends on the backpropagation algorithm and uses a fully connected neural network structure. The method in this paper can effectively solve the problem of gradient disappearance of the backpropagation algorithm, learn more-abstract and high-level feature representation, improve the training effect and generalization ability of the network, and thus improve the accuracy of track circuit fault diagnosis.

4. Conclusions

In light of the complexity of fault types and the low diagnostic precision in jointless track circuit systems, this study advances a fault diagnosis methodology rooted in CWT data preprocessing, DBN feature extraction, and GA-LSSVM classification, utilizing the electrical parameters of indoor and outdoor equipment collected with a centralized monitoring system. The main conclusions are as follows:

- Using the CWT to preprocess the voltage signal data to obtain a wavelet video image is helpful to better capture the dynamic characteristics of the signal, so that the induced voltage signals in different states are easier to distinguish and more interpretable;
- Aiming at the problem of insufficient fault sample data of track circuits, a fault diagnosis model based on optimized DBN-LSSVM is proposed. The DBN exhibits a good feature extraction ability, and the LSSVM has the advantage of solving high-dimensional pattern recognition in the case of small samples, which reduces the working time. The genetic algorithm makes the optimization parameters gradually tend to be optimal with the increase in the number of iterations. Compared with the traditional neural network, this method has better fault diagnosis performance;
- In terms of engineering verification, the proposed model can be applied to an actual track circuit fault diagnosis system to further verify its applicability in practical engineering. The research object of this paper is only the ZPW-2000 track circuit, and a comparative study of 25 Hz phase-sensitive track circuits and high-voltage pulse track circuits can be added in the future.

Author Contributions: Methodology, F.P.; Validation, F.P. and T.L.; Formal analysis, F.P.; Writing—original draft, F.P.; Writing—review & editing, T.L.; Funding acquisition, T.L. All authors have read and agreed to the published version of the manuscript.

Funding: This work was supported in part by the National Natural Science Foundation of China (52172341), the Sichuan Science and Technology Program of China under Grant 2020YFQ0057, the Chongqing Technology Innovation and Application Special Key Project of China under Grant cstc2019jscx-mbdxX0015, and the 2018 "Reliable control and safety maintenance of dynamic systems" project under Grant JDDSTD2018001.

Data Availability Statement: Data are contained within the article.

Conflicts of Interest: The authors declare no conflicts of interest.

Abbreviations

CWT	Continuous wavelet transform
DBN	Deep belief network
RBM	Restricted Boltzmann machine
GA	Genetic algorithm
LSSVM	Least-squares support vector machine
MLP	Multilayer perceptron
BP	Backpropagation neural network
CNN	Convolutional neural network

References

1. Zang, Y.; Shangguan, W.; Cai, B.; Wang, H.; Pecht, M.G. Methods for fault diagnosis of high-speed railways: A review. *Proc. Inst. Mech. Eng. Part O J. Risk Reliab.* **2019**, *233*, 908–922. [CrossRef]
2. Bruin, T.D.; Verbert, K.; Babuka, R. Railway Track Circuit Fault Diagnosis Using Recurrent Neural Networks. *IEEE Trans. Neural Netw. Learn. Syst.* **2016**, *28*, 523–533. [CrossRef]
3. Zhao, B.; Ou, J.; Wang, D.; Jia, Z. Analysis of Transient Response of Jointless Track Circuit Based on Multiconductor Transmission Lines Theory. *IEEJ Trans. Electr. Electron. Eng.* **2022**, *17*, 1570–1579. [CrossRef]
4. Zang, H.; Wang, R. Research on ZPW-2000A Track Circuit State Diagnosis Based on Set Pair Analysis. *IOP Conf. Ser. Earth Environ. Sci.* **2020**, *571*, 012017. [CrossRef]
5. Lu, J.; Yu, J.; Huang, C.; Chen, H. Research on ZPW-2000R Track Circuit Fault Diagnosis Based on Neural Network. *IOP Conf. Ser. Earth Environ. Sci.* **2021**, *693*, 012077. [CrossRef]
6. Gou, L.; Li, H.; Zheng, H.; Li, H.; Pei, X. Aeroengine Control System Sensor Fault Diagnosis Based on CWT and CNN. *Math. Probl. Eng.* **2020**, *2020*, 5357146. [CrossRef]
7. Cao, Y.; Sun, F. Track Circuit Fault Diagnosis Method based on Least Squares Support Vector. *IOP Conf. Ser. Earth Environ. Sci.* **2018**, *108*, 052106. [CrossRef]
8. Zheng, Z.; Dai, S.; Xie, X. Research on Fault Detection for ZPW-2000A Jointless Track Circuit Based on Deep Belief Network Optimized by Improved Particle Swarm Optimization Algorithm. *IEEE Access* **2020**, *8*, 175981–175997. [CrossRef]
9. Chen, J.; Roberts, C.; Weston, P. Fault detection and diagnosis for railway track circuits using neuro-fuzzy systems. *Control Eng. Pract.* **2008**, *16*, 585–596. [CrossRef]
10. Li, J.; Li, G. Research on Fault Diagnosis of ZPW-2000K Track Circuit Based on RS-BN Algorithm. *Teh. Vjesn.-Tech. Gaz.* **2019**, *26*, 1091–1097. [CrossRef]
11. Gao, X.; Wei, H.; Li, T.; Yang, G. A rolling bearing fault diagnosis method based on LSSVM. *Adv. Mech. Eng.* **2020**, *12*, 1687814019899561. [CrossRef]
12. Mao, Z.; Tao, G.; Jiang, B.; Yan, X.G. Adaptive control design and evaluation for multibody high-speed train dynamic models. *IEEE Trans. Control Syst. Technol.* **2020**, *29*, 1061–1074. [CrossRef]
13. Mao, Z.; Yan, X.G.; Jiang, B.; Chen, M. Adaptive fault-tolerant sliding-mode control for high-speed trains with actuator faults and un-certainties. *IEEE Trans. Intell. Transp. Syst.* **2019**, *21*, 2449–2460. [CrossRef]
14. Mao, Z.; Xia, M.; Jiang, B.; Xu, D.; Shi, P. Incipient fault diagnosis for high-speed train traction systems via stacked generalization. *IEEE Trans. Cybern.* **2020**, *52*, 7624–7633. [CrossRef]
15. Fan, Z.; Huang, D.; Xu, K.; Tan, J. Comparative analysis of rail transit braking digital command control strategies based on neural network. *Neural Comput. Appl.* **2023**, *35*, 8833–8845. [CrossRef]
16. Ahmad, S.; Ahmad, Z.; Kim, J.-M. A Centrifugal Pump Fault Diagnosis Framework Based on Supervised Contrastive Learning. *Sensors* **2022**, *22*, 6448. [CrossRef]
17. Ullah, N.; Ahmad, Z.; Siddique, M.F.; Im, K.; Shon, D.-K.; Yoon, T.-H.; Yoo, D.-S.; Kim, J.-M. An Intelligent Framework for Fault Diagnosis of Centrifugal Pump Leveraging Wavelet Coherence Analysis and Deep Learning. *Sensors* **2023**, *23*, 8850. [CrossRef]
18. Zhang, K.; Ma, C.; Xu, Y.; Chen, P.; Du, J. Feature extraction method based on adaptive and concise empirical wavelet transform and its applications in bearing fault diagnosis. *Measurement* **2021**, *172*, 108976. [CrossRef]
19. Wang, X.; Mao, D.; Li, X. Bearing fault diagnosis based on vibro-acoustic data fusion and 1D-CNN network. *Measurement* **2021**, *173*, 108518. [CrossRef]
20. Jia, N.; Cheng, Y.; Liu, Y.; Tian, Y. Intelligent fault diagnosis of rotating machines based on wavelet time-frequency diagram and optimized stacked denoising auto-encoder. *IEEE Sens. J.* **2022**, *22*, 17139–17150. [CrossRef]
21. Xiong, G.; Ma, W.; Zhao, N.; Zhang, J.; Jiang, Z.; Mao, Z. Multi-type diesel engines operating condition recognition method based on stacked auto-encoder and feature transfer learning. *IEEE Access* **2021**, *9*, 31043–31052. [CrossRef]
22. Erkaymaz, O.; Yapici, I.S.; Arslan, R.U. Effects of obesity on time-frequency components of electroretinogram signal using con-tinuous wavelet transform. *Biomed. Signal Process. Control* **2021**, *66*, 102398. [CrossRef]
23. Fischer, A.; Igel, C. An introduction to restricted Boltzmann machines. In *Proceedings of the Progress in Pattern Recognition, Image Analysis, Computer Vision, and Applications: 17th Iberoamerican Congress, CIARP 2012, Buenos Aires, Argentina, 3–6 September 2012*; Proceedings 17; Springer: Berlin/Heidelberg, Germany, 2012; pp. 14–36.

24. Wang, H.; Hu, D. Comparison of SVM and LS-SVM for regression. In Proceedings of the 2005 International Conference on Neural Networks and Brain, Beijing, China, 13–15 October 2005; Volume 1, pp. 279–283.
25. Mirjalili, S.; Seyedali, M. Genetic algorithm. In *Evolutionary Algorithms and Neural Networks: Theory and Applications*; Springer: Berlin/Heidelberg, Germany, 2019; pp. 43–55.